TISSUE ENGINEERING: Part B
Volume 14, Number 3, 2008

DOI: 10.1089/ten.teb.2008.0153

Microcomputed Tomography Characterization of Neovascularization in Bone Tissue Engineering Applications

SIMON YOUNG, D.D.S., Ph.D.,[1] JAMES D. KRETLOW, B.S., B.A.,[1] CHARLES NGUYEN, M.D.,[2] ALEX G. BASHOURA, D.D.S., M.D.,[2] L. SCOTT BAGGETT, Ph.D.,[3] JOHN A. JANSEN, D.D.S., Ph.D.,[4] MARK WONG, D.D.S.,[2] and ANTONIOS G. MIKOS, Ph.D.[1]

ABSTRACT

Vasculogenesis and angiogenesis have been studied for decades using numerous *in vitro* and *in vivo* systems, fulfilling the need to elucidate the mechanisms involved in these processes and to test potential therapeutic agents that inhibit or promote neovascularization. Bone tissue engineering in particular has benefited from the application of proangiogenic strategies, considering the need for an adequate vascular supply during healing and the challenges associated with the vascularization of scaffolds implanted *in vivo*. Conventional methods of assessing the *in vivo* angiogenic response to tissue-engineered constructs tend to rely on a two-dimensional assessment of microvessel density within representative histological sections without elaboration of the true vascular tree. The introduction of microcomputed tomography (micro-CT) has recently allowed investigators to obtain a diverse range of high-resolution, three-dimensional characterization of structures, including renal, coronary, and hepatic vascular networks, as well as bone formation within healing defects. To date, few studies have utilized micro-CT to study the vascular response to an implanted tissue engineering scaffold. In this paper, conventional *in vitro* and *in vivo* models for studying angiogenesis will be discussed, followed by recent developments in the use of micro-CT for vessel imaging in bone tissue engineering research. A new study demonstrating the potential of contrast-enhanced micro-CT for the evaluation of *in vivo* neovascularization in bony defects is described, which offers significant potential in the evaluation of bone tissue engineering constructs.

INTRODUCTION

THE IMPORTANCE of blood vessel formation in the wound healing environment has become increasingly well established over the past few decades. In the past, it was commonly supposed that the formation of new blood vessels in the embryo involved the differentiation of endothelial cells from mesoderm-derived precursor cells (vasculogenesis), while in the adult, new vessels arose solely from preexisting vascular networks through the proliferation and migration of differentiated endothelial cells (angiogenesis).[1] There is increasing evidence, however, that endothelial precursor cells (EPCs) are an essential contributor to adult neovascularization in the settings of ischemia, malignancy, and inflammation.[2] Consequently, Velazquez[3] has attributed neovascularization in the wound healing cascade to events occurring in two separate areas: (1) the remote mobilization of progenitor cells (including EPCs) from the bone marrow in response to various signaling pathways and (2) the action of local factors within

[1]Department of Bioengineering, Rice University, Houston, Texas.
[2]Department of Oral and Maxillofacial Surgery, University of Texas Health Science Center at Houston, Houston, Texas.
[3]Department of Statistics, Rice University, Houston, Texas.
[4]Department of Periodontology and Biomaterials, Radboud University Nijmegen Medical Center, Nijmegen, The Netherlands.

the wound itself, which stimulates angiogenesis from the existing vasculature and promotes the recruitment of circulating bone marrow–derived EPCs that contribute to vasculogenesis. Lastly, the process of arteriogenesis (a process distinct from neovascularization) has been described in the adult as a third mechanism of resolving ischemia from vessel occlusion, in which preexisting small collateral vessels are able to increase their diameter within a very short period of time.[4]

Taking into account conflicting interests, promoting therapeutic neovascularization is an active area of clinical research for the treatment of ischemia (i.e., myocardial infarction[5,6] and limb ischemia[7,8]) and the promotion of wound healing,[9,10] while conditions characterized by excessive or abnormal angiogenesis such as cancer,[11–13] vascular malformations,[14] and wet macular degeneration[15] have also led to numerous efforts to inhibit blood vessel formation.

To determine the therapeutic potential of bioactive factors or cells that may promote or inhibit angiogenesis, an adequate assay system is required. The requirements for an ideal assay of quantitative angiogenesis have been described by Jain *et al.*[16] as the following: (1) the release kinetics and spatio-temporal distribution of the experimental factor are known so that dose–response curves can be calculated; (2) neoplastic cells used as a source of bioactive factors should be genetically characterized with respect to oncogene expression and pro- or antiangiogenic factor production; (3) the structure and function of the new vasculature should be quantifiable; (4) newly formed vessels can be distinguished from preexisting host vessels; (5) tissue damage is avoided to prevent inflammation and its resulting neovascularization; (6) *in vitro* responses can be confirmed *in vivo*; (7) long-term and noninvasive monitoring is possible; and (8) the system is economical, quick, simple, reproducible, and reliable. Not surprisingly, an assay system that meets all of these requirements has not yet been developed. While a wide variety of both *in vitro* and *in vivo* assays exist, there is no standardized measure of angiogenesis, quantification is often absent, and the results are not necessarily applicable to the clinical situation.[17]

EXISTING *IN VITRO* ASSAYS OF ANGIOGENESIS

Many of the essential mechanisms involved in angiogenesis such as endothelial cell proliferation and migration, as well as lumen formation, have been studied using *in vitro* cell culture systems. These provide a useful way to screen potential pro- or antiangiogenic drug therapies. For example, standard proliferation assays such as counting cells with a Coulter counter, or measurements of DNA synthesis through [^{3}H]thymidine incorporation by endothelial cells are readily available. A commonly used cell migration assay utilizes a modified Boyden chamber. Endothelial cells are seeded on top of a cell-permeable membrane and allowed to migrate through in response to a potential chemo-attractant placed below the membrane. Lastly, the differentiation of endothelial cells into tubule-like structures can be studied in both two and three dimensions by culturing endothelial cells on plates coated with Matrigel, collagen, or fibrin.[18] Coculture assays of endothelial cells with dermal fibroblasts[19] and smooth muscle cells[20,21] have also been performed in an attempt to more closely mimic *in vivo* angiogenesis.

Significant limitations to the validity of *in vitro* cell culture assays exist, and the results obtained from such models should be interpreted with caution.[17] These problems include the use of endothelial cells that have undergone multiple passages *in vitro* to achieve sufficient numbers of cells to isolate in culture. Unfortunately, significant phenotypic changes occur over time, such as a change in growth potential. Since endothelial cells are typically quiescent, this may reduce the relevance to the *in vivo* situation. It has also been shown that organ-specific differences exist between microvascular cells, so the response of a cell population to various pro- or antiangiogenic substances can vary depending on the organ source.[22] Compounding these issues, endothelial cells are difficult to maintain *in vitro*. Thus, the effectiveness of antiangiogenic factors in cell proliferation, migration, or tube-formation assays *in vitro* may not accurately represent the *in vivo* situation.

To address the interaction of endothelial cells with both nonendothelial stromal cells and extracellular matrix molecules that occur during *in vivo* angiogenesis, *in vitro* organ culture assays have been developed. The aortic ring assay is an example of one commonly used model in which segments of aorta are dissected from an adult rat and then placed in a matrix-containing environment, such as fibrin.[23] The effect of both pro- or antiangiogenic factors can be tested by quantifying the outgrowth of microvessels from the explant. The advantage of this system is that it allows for more complex interactions to occur while also benefiting from the presence of quiescent cells (as opposed to expanded endothelial cell culture assays) at the beginning of the assay. Angiogenesis, however, is a microvascular event, so the aorta is likely too large a vessel to represent the true *in vivo* situation. Auerbach *et al.*[24] have adapted this model and described the chick aortic arch assay, in which it is claimed that the endothelial cells associated with the embryonic aortic arch are more similar to microvascular endothelial cells, than those from the adult aorta.

The additional level of complexity afforded by such three-dimensional (3D) *in vitro* organ culture assays allows for more realistic predictions of the *in vivo* effect of therapeutic agents while somewhat controlling the level of variability in the system. In spite of this, the aforementioned inadequacies of *in vitro* assays necessitate the use of *in vivo* assays as the next step in validating the effectiveness of a particular factor.

EXISTING *IN VIVO* ASSAYS OF ANGIOGENESIS

One commonly used *in vivo* quantitative angiogenesis assay is the chick chorioallantoic membrane (CAM) assay.[25] Fertilized hen eggs are preincubated for 3 days, and a window is carefully made in the shell and shell membrane. The test factor is loaded into sustained-release polymers, absorbed into gelatin sponges or air-dried onto plastic discs, which are then placed on the CAM, and the window is sealed. Quantification of the effects on angiogenesis is possible by counting the blood vessels within the window, 3–4 days after grafting. The relative simplicity of this assay lends itself to large-scale screening of therapeutic compounds, although results may be confounded by misinterpretation of normal morphological changes in the rapidly growing CAM vascular network.[17] Additional variability may occur if CAM irritants such as shell dust are generated during the initial window cutting procedure (which can lead to an inflammatory response) or if the window is not resealed properly after initial implantation (the CAM is sensitive to changes in oxygen tension).[17] Lastly, monitoring of the test area window *in ovo* can be difficult, although a variation of this technique has been described by Auerbach *et al*.,[26] in which the embryos are explanted from their shells and cultured in Petri dishes. This modification allows for multiple grafts to be placed on the CAM *in vitro*, as well as continuous monitoring of the response.

The corneal micropocket model is another frequently utilized *in vivo* angiogenesis assay. Introduced in 1974 by Gimbrone *et al.*,[27] this method was originally developed for rabbits, although it has been adapted for both rats[28] and mice.[29] An advantage of the corneal angiogenesis assay over the CAM assay is that the cornea is avascular. As a result, when proangiogenic factors are introduced into the corneal pocket, any vessels that enter the site from the adjacent limbal vasculature are new, thus eliminating the problem of differentiating new from preexisting blood vessels during quantitative analysis. The angiogenic response can be monitored both *in vivo* using a slit lamp or stereomicroscope, as well as histologically. An additional advantage of this assay in mice is that it can take advantage of the wealth of inbred strains and transgenic animals available for testing.[30] Interestingly, the normal avascularity of this model has also been cited as a disadvantage, using the rationale that angiogenesis *in vivo* does not normally occur in avascular regions, and the implantation site lacks accessibility to factors in the bloodstream, which might normally influence vessel formation.[24]

The corneal micropocket assays are technically demanding, and investigators face the ethical dilemma of utilizing an assay that compromises a major sensory organ. Subcutaneous implantation of matrix-implants is relatively easier to perform, and several carriers have been utilized to deliver therapeutic agents such as sponge disks,[31] Matrigel,[32] or semiclosed silicon cylinders.[33] Following implantation, granulation tissue is formed, and new vessels invade the carrier. Implants are removed 1–3 weeks later, and angiogenesis is quantified by morphometric analysis of histological sections[34–36] or through the use of spectrophotometry to measure the volume of fluorescein isothiocyanate-dextran–injected vessels generated within an implant.[33]

While the use of histological sections is the current standard for quantifying angiogenesis *in vivo*, it does not permit noninvasive, continuous monitoring of the angiogenic response and is limited to fixed time points. Chamber assays such as the dorsal skin fold chamber[37] and rabbit ear chamber[38] typically consist of a transparent chamber containing the experimental agent and exposed subcutaneous tissue, allowing long-term *in vivo* monitoring of angiogenic effects through intravital microscopy. Since vessel growth can be monitored continuously in a single animal, multiple animals assessed at different time points are unnecessary. Attempts to further simplify the process of chamber assays for drug screening have prompted investigators to develop simpler whole animal models such as the zebrafish embryo assay.[39]

The zebrafish is a small tropical fish that has a short gestational period, is easily and inexpensively maintained at high densities, and has organs that are remarkably similar to those in humans at the anatomical, physiological, and molecular levels.[40] The development of blood vessels in the zebrafish embryo has been well characterized, and the optical transparency of the embryos allows for direct and continuous microscopic observations on the effects of pro- and anti-angiogenic agents. Three-dimensional quantification of angiogenesis using fluorescent markers and confocal microscopy is also possible with this assay. Recent applications of this technology include studies on tumor cell metastasis, the induction of angiogenesis, and subsequent tumor cell–vascular interactions.[41]

THE ASSESSMENT OF ANGIOGENESIS IN BONE TISSUE ENGINEERING STUDIES

As can be seen from this brief review of angiogenesis assays, *in vitro* tests provide useful information as a first step in validating a therapeutic agent, but the additional physiological complexities provided by *in vivo* models are required to more accurately evaluate preclinical effectiveness. Many of the *in vivo* models discussed have been used to test applications related to diseases such as cancer (antiangiogenic agents) or cardiovascular ischemia (proangiogenic agents). These same assays can be used in the emerging field of tissue engineering to investigate the effects of various bioactive factors. In fact, Laschke *et al.*[37] have stated that "delayed vascularization or lack of vascularization is one of the major obstacles to successfully realizing the clinical use of *in vitro* engineering tissue and organ substitutes." Bone tissue

engineering in particular is an excellent candidate for the use of proangiogenic factors, considering the critical role angiogenesis plays in bone regeneration.[42] To date, several recombinant angiogenic growth factors, such as vascular endothelial growth factor (VEGF),[43] platelet-derived growth factor (PDGF),[44] and fibroblast growth factor-2 (FGF-2), have been used to encourage bone healing in animal models.[45]

Traditionally, parameters such as microvessel density and average capillary area have been used to assess angiogenesis within histological sections of healing bone defects. This method yields a two-dimensional (2D) approximation of the 3D vascular network associated with an implanted tissue engineering scaffold, prompting investigation into the use of 3D imaging modalities such as microcomputed tomography (micro-CT). Micro-CT has already been used to characterize the coronary,[46] hepatic,[47] and renal[48,49] microvasculature of small rodents, as well as of collateral vessel formation in mouse hind limb ischemia models.[50,51] In addition, micro-CT is rapidly becoming a common method to quantify bone formation *in vivo*.[43,52–54] Few studies, however, have utilized micro-CT to examine vessel formation during bone healing.

Micro-CT as a means of characterizing angiogenesis in bone tissue engineering

At present, only two studies have reported the use of micro-CT to quantify the vasculature associated with tissue engineering scaffolds implanted in a healing bone defect.[55,56]

Rai *et al.*[56] used micro-CT to study the angiogenic and osteogenic effect of poly(ε-caprolactone)-tricalcium phosphate (PCL-TCP) composite scaffolds loaded with platelet-rich plasma (PRP) in rat femoral segmental defects. For the evaluation of vascularization, animal subjects were euthanized at 3 weeks postimplantation and perfused via the abdominal aorta with Microfil, a proven silicone-based vascular contrast agent for micro-CT studies.[50,56,57] The samples were subsequently fixed and decalcified. Quantitative assessment of the vasculature was performed by measuring the vascular volume fraction (VVF), which the authors defined as the fraction of the volume of interest (VOI) that was vascularized. It was found that PRP-loaded PCL-TCP scaffolds had a 70.3% higher VVF than empty PCL-TCP control scaffolds. Additional imaging in the form of 3D micro-CT models illustrated the effect of PRP on early vascularization by displaying the enhanced vascularity of the PRP-treated group versus controls.

Patel *et al.*[55] also utilized contrast-enhanced micro-CT to quantify the effect of controlled growth factor release on vessel formation within a rat cranial cavitational defect. Porous poly(propylene fumarate) (PPF) scaffolds were loaded with gelatin microparticles containing phosphate-buffered saline, VEGF alone, bone morphogenetic protein-2 (BMP-2) alone, or both VEGF and BMP-2. These composite scaffolds were then implanted into critical-size cranial defects and examined for neovascularization using micro-CT at 4 weeks. Similar to the protocol utilized by Rai *et al.*,[56] animals were perfused postmortem with Microfil, and the samples harvested, fixed, and decalcified to enable micro-CT analysis of vessel formation. The percent blood vessel volume at 4 weeks was found to be highest in the VEGF-treated group, although this result was not statistically significant.

These two aforementioned studies illustrate the ability of contrast-enhanced micro-CT imaging to provide both quantitative and qualitative information on the neovascularization of implanted bone tissue engineering constructs. Recent work has also led to the application of this micro-CT–based method toward the characterization of the vascular response associated with a healing rabbit alveolar bone defect. Indeed, both long bone segmental defect[52,58,59] and cranial cavitational defect[60–63] models are commonly performed in small rodents to test bone regeneration materials. However, to provide a reproducible and challenging test bed for potential bone tissue engineering constructs in the unique healing environment of the oral cavity, a rabbit alveolar bone nonhealing defect model has recently been developed.[64] Both histological characterization of wound healing and micro-CT quantification of bone repair within this rabbit model have been performed at 8 and 16 weeks.[64] Thus, by introducing a 3D method for quantifying neovascularization in this defect model, investigators would have the expanded ability to quantitatively assess both the angiogenic and osteogenic potential of an implanted biomaterial in a clinically relevant environment.

To test the applicability of the contrast-enhanced micro-CT protocol for studying angiogenesis in the rabbit alveolar bone model, porous PPF scaffolds were implanted into the defects and compared with their empty controls. Both 2- and 4-week time points were chosen to observe quantitative changes in vascularization occurring within the healing defect, resulting in four groups: (1) empty defect at 2 weeks; (2) implanted defect at 2 weeks; (3) empty defect at 4 weeks; and (4) implanted defect at 4 weeks. Following euthanasia, postmortem bilateral injections of the carotid arteries with Microfil were carried out on all groups (Figs. 1 and 2), and the samples were harvested, fixed, and decalcified as previously described.[50,55,56]

As previously reported,[50,55,56] the percent vascularization (PV) within each VOI was calculated as follows:

$$\%\ \text{vascularization} = \frac{\text{vessel volume } (\mu m^3)}{\text{VOI volume } (\mu m^3)} \times 100\%$$

Considering that the implanted porous PPF scaffolds were expected to undergo minimal to no degradation, the % vascularization within the VOI of the implanted groups could never reach 100%. Thus, a standardized percent vascularization (SPV) was also calculated, which took this issue into consideration.

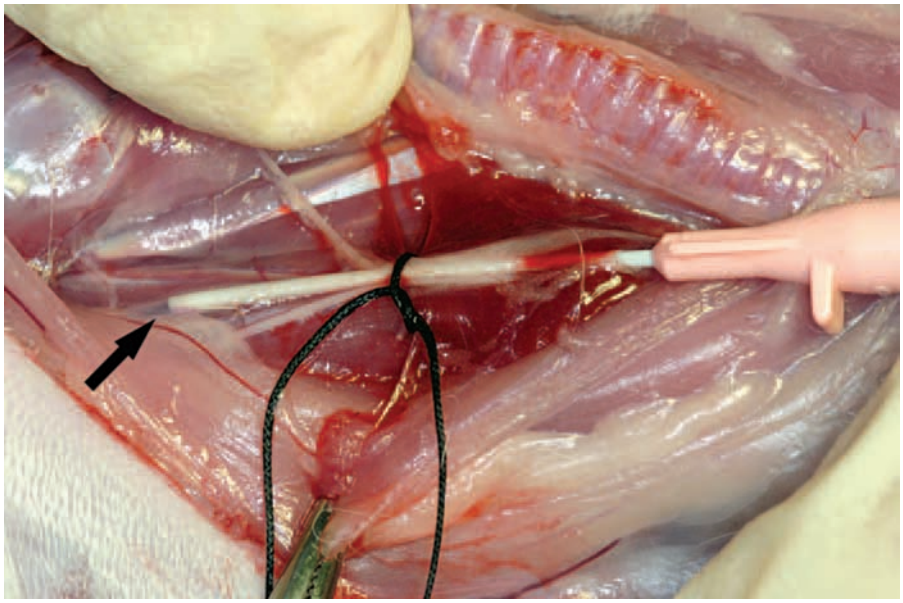

FIG. 1. Intraoperative photo of the postmortem Microfil perfusion procedure. The neck of the rabbit has been dissected to expose the carotid sheath. The black arrow points to the tip of an angiocatheter that has been placed within the lumen of the internal carotid artery.

$$\text{standardized \% vascularization} = \frac{\text{vessel volume}\,(\mu m^3)}{\text{VOI volume}\,(\mu m^3) - \text{average volume of PPF per scaffold}\,(\mu m^3)} \times 100\%$$

In addition to calculating vessel volume within the healing defects, the average vessel thickness (AVT) within the VOI of each animal specimen was determined, including a histogram of the vessel size distribution similar to that shown by Duvall *et al.*[50] According to the manufacturer, the micro-CT software (CT-Analyzer; Skyscan, Aartselaar, Belgium) determines average thickness as an average of the ''local thickness'' at each binarized voxel representing Microfil-perfused vessels. The local thickness is defined as the diameter of a sphere that fulfils two conditions: (1) the sphere encloses the binarized voxel (but the binarized voxel is not necessarily the centre of the sphere); (2) the sphere is entirely bounded within the binarized solid surfaces.

The empty defect group at 2 weeks had a mean PV of $5.29\% \pm 0.80\%$ as compared to the PPF-implanted defect

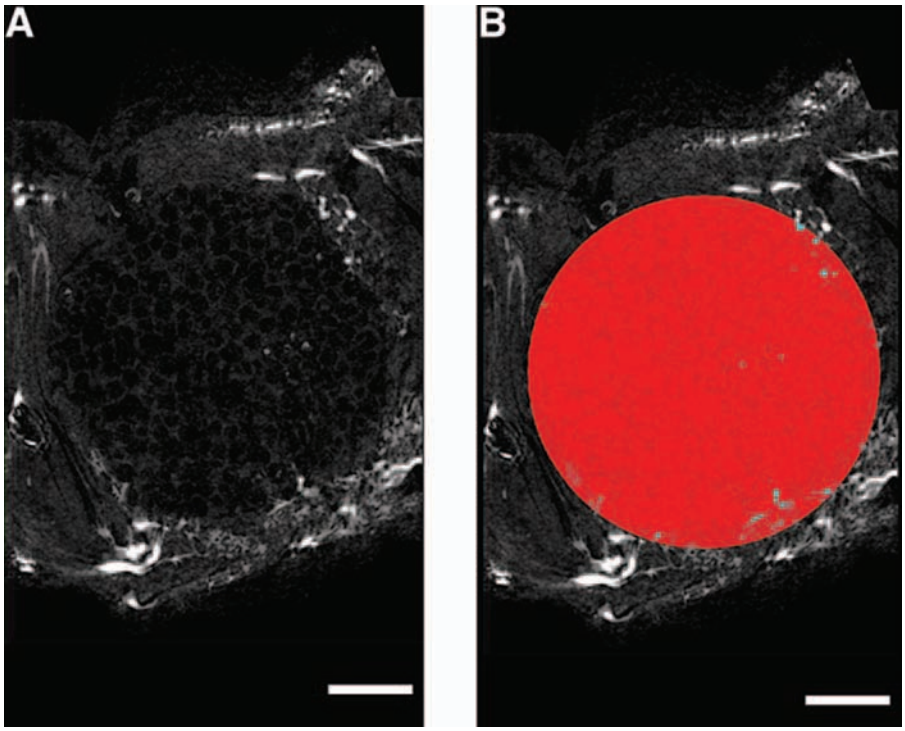

FIG. 2. Illustration of the VOI used to analyze the rabbit alveolar bone defect. (**A**) Representative sagittal 2D ''slice'' through a scaffold-implanted alveolar bone defect. Note that the blood vessels appear as bright spots. (**B**) A circular 10 mm diameter VOI is drawn and extended through the depth of the defect to create the geometry of the original bone defect. Bar represents 2 mm in both images.

group's mean PV of $1.58\% \pm 0.24\%$ at 2 weeks. At 4 weeks, the empty defect group had a mean PV of $7.18\% \pm 1.04\%$, compared to a PV of $2.83\% \pm 0.75\%$ for the PPF-implanted group at the same time point. Thus, a 3.3- and 2.5-fold decrease in vascularity was observed when comparing empty control groups to PPF-implanted groups at 2 and 4 weeks, respectively. The differences in PV between the control and PPF-implanted groups were significant at the $p < 0.05$ level for both 2- and 4-week time points (Fig. 3). While an increase in vascularity was observed from 2 to 4 weeks in both the empty control and PPF-implanted groups, the differences were not significant.

At 2 weeks, the PV of the control group was 2.2-fold greater than the SPV of the PPF-implanted group ($2.43\% \pm 0.37\%$), while the PV of the control group at 4 weeks was 1.6-fold greater than the SPV of the PPF-implanted group at the same time point ($4.58\% \pm 1.31\%$). Accordingly, the fold-decrease in vascularization for empty versus PPF-implanted groups was reduced using SPV for comparison (Fig. 4).

Thus, at both 2- and 4-week time points, quantitative micro-CT analysis of the vessel network showed a decreased PV and SPV for the PPF-implanted defects versus empty controls (Figs. 3 and 4). Although a direct comparison of vascularization between a scaffold-implanted defect and an empty control was not the main intent of this study, it was nonetheless important to test the ability of this method to detect and quantify differences in vessel formation between different treatments, especially considering the potential of this model as a test bed for both angiogenic and osteogenic biomaterials.

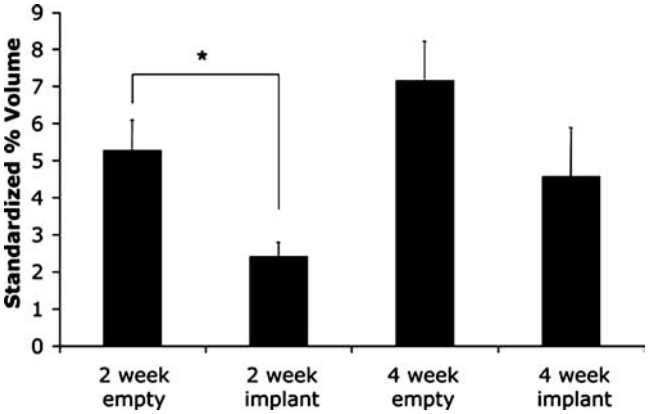

FIG. 4. Results of micro-CT quantitative analysis of standardized percent vascularization (SPV) for an empty control and a scaffold-implanted alveolar bone defect examined at 2 and 4 weeks. Error bars designate mean ± standard error. The number of repetitions for each group is $n = 6$. Asterisk indicates statistically significant difference ($p < 0.05$) in SPV between the control and PPF-implanted groups at 2 weeks.

For comparison, although no unimplanted control subjects were examined in their study, Rai *et al.*[56] reported a $0.97\% \pm 0.10\%$ vessel volume fraction for empty PCL-TCP control scaffolds. Similarly, Patel *et al.*[55] reported a $1.64\% \pm 0.73\%$ vessel volume for unloaded PPF scaffolds, and a vascular volume of $1.81\% \pm 1.27\%$ for empty defects. These results are similar in magnitude to the PV of the PPF-implanted groups in this rabbit alveolar bone defect study at

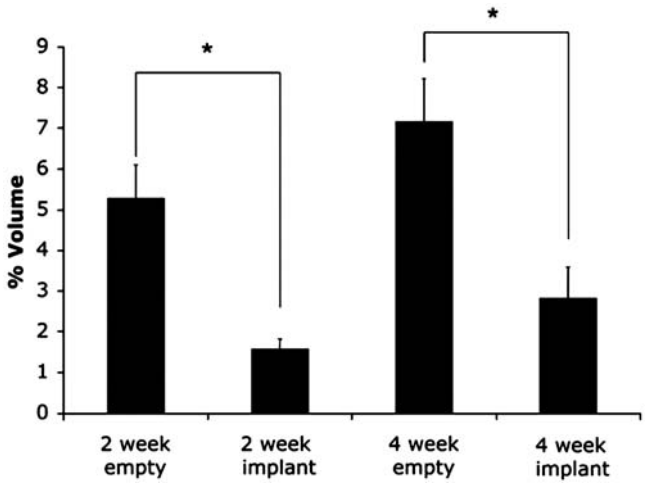

FIG. 3. Results of micro-CT quantitative analysis of percent vascularization (PV) for an empty control and a scaffold-implanted rabbit alveolar bone defect examined at 2 and 4 weeks. Error bars designate mean ± standard error. The number of repetitions for each group is $n = 6$. Asterisks indicate statistically significant difference ($p < 0.05$) in PV between the 2-week PPF-implanted and control groups, as well as the 4-week PPF-implanted and control groups.

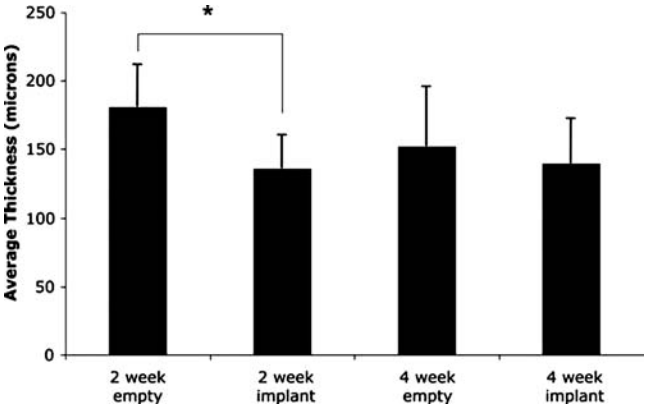

FIG. 5. Results of micro-CT quantitative analysis of average vessel thickness (AVT) for an empty control and a scaffold-implanted alveolar bone defect examined at 2 and 4 weeks. Error bars designate mean ± standard error. The number of repetitions for each group is $n = 6$. Asterisk indicates statistically significant difference ($p < 0.05$) in AVT between the PPF-implanted and control groups at 2 weeks.

2 and 4 weeks, which were $1.58\% \pm 0.24\%$ and $2.83\% \pm 0.75\%$, respectively.

Quantitative micro-CT analysis also revealed differences in AVT amongst the four groups of this study (Fig. 5). The empty control group at 2 weeks had an AVT of $180.8 \pm 7.2\,\mu m$, while AVT decreased at 4 weeks to $151.8 \pm 10.3\,\mu m$ in the control group. It is possible that remodeling of the vascular network occurred in the wound healing environment between the two time points examined, and that a more mature vessel network was present by week 4 in empty control defects. Similar observations have been reported by Niimi,[65] who found that the diameter of small neocapillaries was reduced between 2- and 4-week time points in a mouse cerebral ischemia model testing both PDGF and FGF-2 as therapeutic agents. The author of that paper explained these results by noting that newly formed capillaries are wide, tortuous, and fragile, and that the process of sprouting angiogenesis results in a gradual widening and extension of the capillary lumen until it contacts another capillary where it makes a connection. Thus, the micro-CT analysis of AVT in a healing rabbit alveolar bone defect suggests the presence of an immature vessel network present at 2 weeks, with subsequent remodeling seen by 4 weeks.

To our knowledge, there are no studies that have examined how the presence of a scaffold influences vessel network morphology (as measured three-dimensionally by micro-CT) within a healing bone defect. The present study showed that the PPF-implanted groups had a decreased AVT as compared to their empty controls at comparable time points (Fig. 5). The most similar study that could be found in the literature was conducted by Druecke *et al.*,[66] who examined the vascularization of porous poly(ether ester) block copolymer scaffolds within a mouse skinfold chamber. In that study, it was found that scaffolds at 20 days postimplantation with a pore size of 250–300 μm had a larger average vessel diameter (approx. 12 μm) than those with a pore size of 20–75 μm (10.11 μm). The surrounding "control" tissue had an average vessel diameter between 6 and 7 μm. While it is tempting to compare the AVT data between the present study and that by Druecke *et al.*,[66] the physiologic environment of the two studies differed, as did the material implanted and the method of quantification (3D micro-CT versus 2D fluorescence microscopy).

The last quantifiable characteristic of the vessel network that was examined in the present study was the vessel size distribution. As can be seen in Figure 6, the majority of vessels had a diameter ranging from 45 to 226 μm, regardless of experimental group. A similar vessel size distribution histogram was published by Duvall *et al.*,[50] in which a large proportion of the blood vessel size distribution in the control limbs of a mouse ischemia model was in the 100–400 μm range. While limited comparisons of the vessel thickness distribution in a healing rabbit alveolar bone defect can be made to that of a mouse hind limb, it seems that these results are consistent with each other and suggest that a major proportion of the newly formed vessel network associated with the bony defect is larger in diameter than the typical capillary.

In addition to the quantitative measures used in this study to characterize neovascularization, qualitative data from both maximum intensity projection (MIP) images and 3D models provided useful information to assist in evaluating the morphology of the vessel network throughout the volume of the empty bone defect or implanted PPF scaffold.

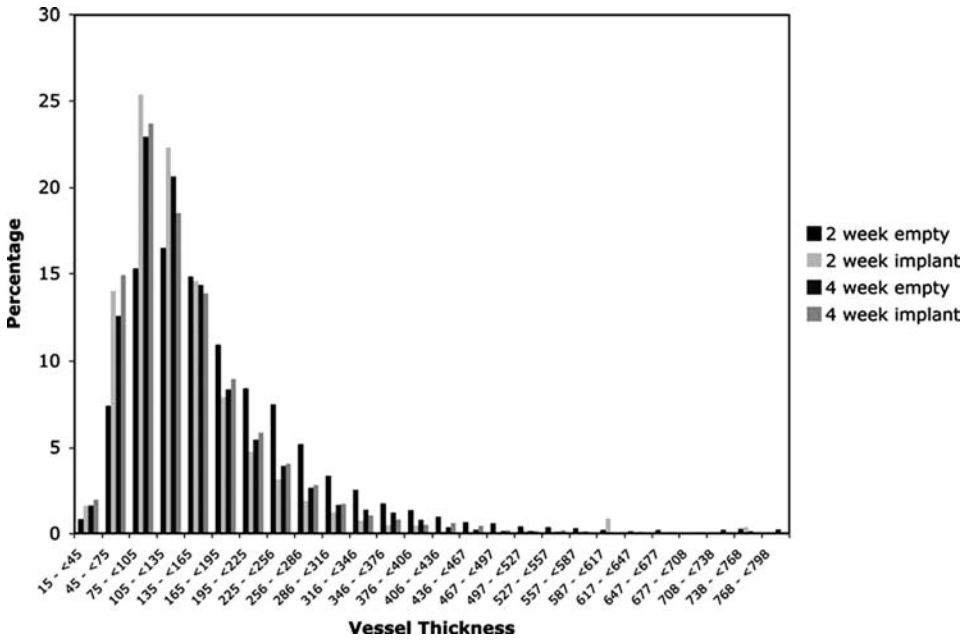

FIG. 6. Micro-CT–generated distribution of vessel thickness (in microns) for an empty control and a scaffold-implanted alveolar bone defect examined at 2 and 4 weeks. The number of repetitions for each group is $n = 6$.

MIPs are a visualization method for 3D data that project the voxels with maximum intensity (i.e., the brightest) that fall along parallel rays traced from the viewpoint to the plane of projection. In short, an MIP is a 2D projection of the brightest voxels in a 3D data set, and is dependent on the given viewing direction (a more detailed review of the use of MIPs in computed tomographic angiography has been written by Prokop *et al.*[67]). By providing a computationally fast way to generate pseudo-3D images of the vasculature, MIPs are a convenient method of preliminary assessment of vessel network morphology prior to 3D modeling. While quantitative analysis is not possible using MIPs to compare the vascular volume, these coronally oriented images illustrate the pattern of vessel in-growth for both the empty control groups and PPF-implanted groups (Fig. 7). The MIPs of both control groups at 2 and 4 weeks showed an abundant neovasculature traversing the full width of the healing alveolar bone defects, while the MIPs of PPF-implanted groups at 2 and 4 weeks displayed a markedly reduced density of vessels at the center of the PPF implants. The 3D models generated for all four groups revealed the same pattern of reduced vascularity for the PPF-implanted groups, most notably in the center of the VOI (Fig. 8). These imaging results suggest that sprouting angiogenesis was initiated at the buccal and lingual borders of the alveolar bone defect and that the presence of an implant affected the centripetal progression of neovascularization toward the center of the defect.

While the current study and those by Rai *et al.*[56] and Patel *et al.*[55] have illustrated the ability of micro-CT imaging to generate both quantitative and qualitative measures of neovascularization in both empty and scaffold-implanted bone defects, several limitations of the technique should be kept in mind. As in any trauma-inducing situation, surgical manipulation leads to cell damage, which in turn, induces an inflammatory reaction. Since several proangiogenic cytokines are released by cells involved in the inflammatory response, care must be taken to minimize

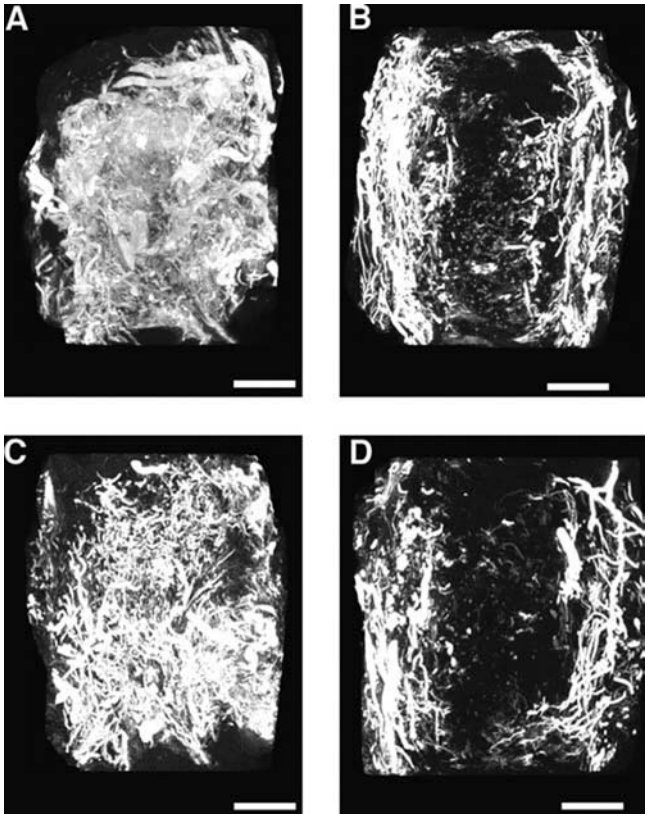

FIG. 7. Micro-CT–generated representative coronally oriented MIP images. Note that the buccal and lingual aspects of each alveolar bone defect are, respectively, shown on the right and left of each image. (**A**) Empty control defect at 2 weeks. (**B**) Scaffold-implanted defect at 2 weeks. (**C**) Empty control defect at 4 weeks. (**D**) Scaffold-implanted defect at 4 weeks. Bar represents 2 mm in all images.

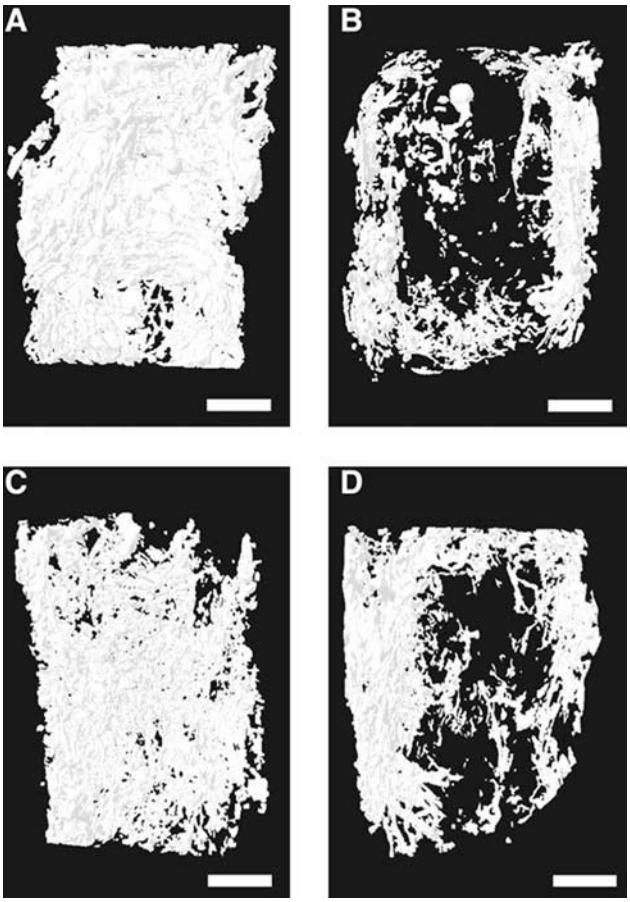

FIG. 8. Micro-CT–generated representative 3D models of the vessel network associated with the alveolar bone defect. Note that the buccal and lingual aspects of each defect are, respectively, shown on the right and left of each image. (**A**) Empty control defect at 2 weeks. (**B**) Scaffold-implanted defect at 2 weeks. (**C**) Empty control defect at 4 weeks. (**D**) Scaffold-implanted defect at 4 weeks. The differences in vessel architecture seen in these 3D models when comparing empty controls to scaffold-implanted groups correspond well to that seen using MIP images. Bar represents 2 mm in all images.

surgical trauma to the tissues involved, and test samples must be compared to vehicle-exposed counterparts to allow reliable interpretation of the data.[68]

Any perfusion-based technique assumes that the contrast agent completely fills the vasculature and does not leak into the surrounding tissues. This might not always be true as Patel *et al.*[55] found in histological sections of Microfil-perfused specimens, where some blood vessels were incompletely filled. Less viscous agents such as barium sulfate might be expected to fill vessels more effectively, but in a comparative study by Duvall *et al.*,[50] Microfil was found to be a superior contrast agent because of its homogeneous coefficient of attenuation within vessels and more effective vascular filling. A disadvantage of Microfil reported by the same authors was the similar attenuation coefficient to bone. This lack of contrast required decalcification of samples before the vasculature could be properly analyzed. The same study found excellent correlation between micro-CT–based and histological methods of establishing the ratio of arterioles in the surgery limb to the control limb.

Grabherr *et al.*[69] recently provided an excellent review of historic and current contrast agents used in postmortem angiography. In brief, the authors categorized these agents as corpuscular preparations, oily liquids, hydrosoluble preparations, or casts. Corpuscular preparations such as barium sulfate contain radiopaque particles that are typically water-soluble. While such preparations allow for imaging of the microcirculation, this ability may be solvent dependent (i.e., certain barium sulfate preparations enter capillaries when dissolved in water, but not in gelatin). Additional disadvantages of corpuscular preparations include imaging artifacts due to precipitation of the radiopaque particles within vessels, and extravasation of the agents when dissolved in water. Oily contrast agent liquids, like the corpuscular preparations, allow for high-contrast angiographic images. While the oily liquids are retained by vessels for longer periods without extravasation, as compared to corpuscular preparations, their ability to penetrate the microcirculation is viscosity dependent. The hydrosoluble preparations are easily injectable and essential for *in vivo* imaging, but rarely used in postmortem angiography since they rapidly diffuse through vessel walls, and contribute a relatively poor amount of radiopacity. Lastly, casting materials are described as radiopaque materials that are injected into the vascular system, and subsequently harden. The silicon rubber–lead oxide technique is the most common method in use (Microfil being an example of such a material), with the advantages of having less imaging artifacts and a lack of vessel extravasation upon hardening. While the disadvantages of casting materials such as polymerization shrinkage may affect micro-CT measurements (i.e., AVT), the inability of flushing out the material after imaging is less of a concern.

Unlike other *in vivo* assays of angiogenesis such as the CAM, zebrafish, or chamber assays, the use of Microfil perfusion and *ex vivo* micro-CT scanning of harvested samples does not allow for continuous, noninvasive monitoring of vascularization at different time points in the same animal. However, these aforementioned assays cannot be used for testing bone tissue engineering constructs. High-resolution *in vivo* micro-CT scans performed on anesthetized animals may be an alternative, although segmentation of the vasculature from the surrounding hard tissues would be necessary to evaluate angiogenesis in bone tissue engineering applications. In addition, the spatial resolution of *in vivo* micro-CT on living animals typically cannot match that of *ex vivo* or *in vitro* micro-CT due to blurring from cardiac and respiratory motion during image acquisition. To address such concerns, the use of stereotactic devices for head immobilization during rodent cerebral vasculature imaging has been reported,[70] as well as the use of cardiac- and respiratory-gated micro-CT for imaging of the mouse heart.[71] With the continued advancement of *in vivo* micro-CT technology, sub-100 μm resolution *in vivo* vascular imaging may soon become a reality.

CONCLUSIONS

Assays of neovascularization have proven useful for studying the mechanisms involved in angiogenesis, and also for testing potential therapeutic agents, whether they are anti-angiogenic for treating cancer, or proangiogenic for the treatment of cardiovascular ischemia. While several *in vitro* systems exist for screening compounds of interest, *in vivo* assays are necessary to confirm therapeutic effectiveness. The systems currently in use each have their advantages and limitations, but the measurement of microvessel density in histological sections has traditionally been the gold standard for evaluating the vascular response to bone tissue engineering constructs. Contrast agent–enhanced micro-CT shows promise as a method of providing nondestructive, 3D analysis of neovascularization occurring within a healing bone defect. Both quantitative and qualitative methods of micro-CT analysis can be used to establish the unique morphological characteristics of a newly formed vascular network associated with both empty and scaffold-implanted bone defects. Accordingly, the preliminary results using this methodology in a variety of animal models and defect locations demonstrate its potential to evaluate the angiogenic effect of tissue engineering constructs placed within a wide variety of *in vivo* models, as long as perfusion is possible.

ACKNOWLEDGMENTS

This work has been supported by the National Institutes of Health (R01 DE15164). Simon Young also gratefully acknowledges financial support from a Research Fellow-

ship given by the Oral and Maxillofacial Surgery Foundation. James D. Kretlow also acknowledges support by the National Institutes of Health and Rice University Institute of Biosciences and Bioengineering (T32 GM008362). J.D.K. is a student in the Baylor College of Medicine Medical Scientist Training Program and was also supported by the National Institute of General Medical Sciences (T32 GM07330).

REFERENCES

1. Bauer, S.M., Bauer, R.J., and Velazquez, O.C. Angiogenesis, vasculogenesis, and induction of healing in chronic wounds. Vasc. Endovascular Surg. **39,** 293, 2005.
2. Carmeliet, P. Angiogenesis in health and disease. Nat. Med. **9,** 653, 2003.
3. Velazquez, O.C. Angiogenesis and vasculogenesis: inducing the growth of new blood vessels and wound healing by stimulation of bone marrow-derived progenitor cell mobilization and homing. J. Vasc. Surg. **45 Suppl A,** A39, 2007.
4. Buschmann, I., Katzer, E., and Bode, C. Arteriogenesis—is this terminology necessary? Basic Res. Cardiol. **98,** 1, 2003.
5. Schachinger, V., Assmus, B., Britten, M.B., Honold, J., Lehmann, R., Teupe, C., Abolmaali, N.D., Vogl, T.J., Hofmann, W.K., Martin, H., Dimmeler, S., and Zeiher, A.M. Transplantation of progenitor cells and regeneration enhancement in acute myocardial infarction: final one-year results of the TOPCARE-AMI Trial. J. Am. Coll. Cardiol. **44,** 1690, 2004.
6. Schueller, P.O., Meyer, C., Brehm, M., Wernet, P., Schannwell, C.M., and Strauer, B.E. Intracoronary autologous bone marrow cell transplantation beneficially modulates heart rate variability. Int. J. Cardiol. **119,** 398, 2007.
7. Marui, A., Tabata, Y., Kojima, S., Yamamoto, M., Tambara, K., Nishina, T., Saji, Y., Inui, K., Hashida, T., Yokoyama, S., Onodera, R., Ikeda, T., Fukushima, M., and Komeda, M. A novel approach to therapeutic angiogenesis for patients with critical limb ischemia by sustained release of basic fibroblast growth factor using biodegradable gelatin hydrogel: an initial report of the phase I-IIa study. Circ. J. **71,** 1181, 2007.
8. Mikroulis, D., Papanas, N., Maltezos, E., and Bougioukas, G. Angiogenic growth factors in the treatment of peripheral arterial disease. Curr. Vasc. Pharmacol. **5,** 195, 2007.
9. Steed, D.L. Clinical evaluation of recombinant human platelet-derived growth factor for the treatment of lower extremity ulcers. Plast. Reconstr. Surg. **117,** 143S, 2006.
10. Cianfarani, F., Tommasi, R., Failla, C.M., Viviano, M.T., Annessi, G., Papi, M., Zambruno, G., and Odorisio, T. Granulocyte/macrophage colony-stimulating factor treatment of human chronic ulcers promotes angiogenesis associated with *de novo* vascular endothelial growth factor transcription in the ulcer bed. Br. J. Dermatol. **154,** 34, 2006.
11. Papageorgio, C., and Perry, M.C. Epidermal growth factor receptor-targeted therapy for pancreatic cancer. Cancer Invest. **25,** 647, 2007.
12. Delongchamps, N.B., and Peyromaure, M. The role of vascular endothelial growth factor in kidney and prostate cancer. Can. J. Urol. **14,** 3669, 2007.
13. Banerjee, S., Dowsett, M., Ashworth, A., and Martin, L.A. Mechanisms of disease: angiogenesis and the management of breast cancer. Nat. Clin. Pract. **4,** 536, 2007.
14. Hashimoto, T., Emala, C.W., Joshi, S., Mesa-Tejada, R., Quick, C.M., Feng, L., Libow, A., Marchuk, D.A., and Young, W.L. Abnormal pattern of Tie-2 and vascular endothelial growth factor receptor expression in human cerebral arteriovenous malformations. Neurosurgery **47,** 910, 2000.
15. Kourlas, H., and Abrams, P. Ranibizumab for the treatment of neovascular age-related macular degeneration: a review. Clin. Ther. **29,** 1850, 2007.
16. Jain, R.K., Schlenger, K., Hockel, M., and Yuan, F. Quantitative angiogenesis assays: progress and problems. Nat. Med. **3,** 1203, 1997.
17. Auerbach, R., Akhtar, N., Lewis, R.L., and Shinners, B.L. Angiogenesis assays: problems and pitfalls. Cancer Metastasis Rev. **19,** 167, 2000.
18. Ucuzian, A.A., and Greisler, H.P. *In vitro* models of angiogenesis. World J. Surg. **31,** 654, 2007.
19. Bishop, E.T., Bell, G.T., Bloor, S., Broom, I.J., Hendry, N.F., and Wheatley, D.N. An *in vitro* model of angiogenesis: basic features. Angiogenesis **3,** 335, 1999.
20. Korff, T., Kimmina, S., Martiny-Baron, G., and Augustin, H.G. Blood vessel maturation in a 3-dimensional spheroidal coculture model: direct contact with smooth muscle cells regulates endothelial cell quiescence and abrogates VEGF responsiveness. FASEB J. **15,** 447, 2001.
21. Heydarkhan-Hagvall, S., Helenius, G., Johansson, B.R., Li, J.Y., Mattsson, E., and Risberg, B. Co-culture of endothelial cells and smooth muscle cells affects gene expression of angiogenic factors. J. Cell. Biochem. **89,** 1250, 2003.
22. Auerbach, R. Vascular endothelial cell differentiation: organ-specificity and selective affinities as the basis for developing anti-cancer strategies. Int. J. Radiat. Biol. **60,** 1, 1991.
23. Go, R.S., and Owen, W.G. The rat aortic ring assay for *in vitro* study of angiogenesis. Methods Mol. Med. **85,** 59, 2003.
24. Auerbach, R., Lewis, R., Shinners, B., Kubai, L., and Akhtar, N. Angiogenesis assays: a critical overview. Clin. Chem. **49,** 32, 2003.
25. Storgard, C., Mikolon, D., and Stupack, D.G. Angiogenesis assays in the chick CAM. Methods Mol. Biol. **294,** 123, 2005.
26. Auerbach, R., Kubai, L., Knighton, D., and Folkman, J. A simple procedure for the long-term cultivation of chicken embryos. Dev. Biol. **41,** 391, 1974.
27. Gimbrone, M.A., Jr., Cotran, R.S., Leapman, S.B., and Folkman, J. Tumor growth and neovascularization: an experimental model using the rabbit cornea. J. Natl. Cancer Inst. **52,** 413, 1974.
28. Schwartz, S., George, J., Ben-Shoshan, J., Luboshits, G., Avni, I., Levkovitch-Verbin, H., Ziv, H., Rosner, M., and Barak, A. Drug modification of angiogenesis in a rat cornea model. Invest. Ophthalmol. Vis. Sci. **49,** 250, 2008.
29. Rogers, M.S., Birsner, A.E., and D'Amato, R.J. The mouse cornea micropocket angiogenesis assay. Nat. Protoc. **2,** 2545, 2007.
30. Muthukkaruppan, V., and Auerbach, R. Angiogenesis in the mouse cornea. Science **205,** 1416, 1979.
31. Kim, C.D., Kim, H.H., Kim, Y.K., Kwak, Y.K., Kim, S., Yoo, S., and Hong, K.W. Antiangiogenic effect of KR31372 in rat sponge implant model. J. Pharmacol. Exp. Ther. **296,** 1085, 2001.

32. Passaniti, A., Taylor, R.M., Pili, R., Guo, Y., Long, P.V., Haney, J.A., Pauly, R.R., Grant, D.S., and Martin, G.R. A simple, quantitative method for assessing angiogenesis and antiangiogenic agents using reconstituted basement membrane, heparin, and fibroblast growth factor. Lab. Invest. **67,** 519, 1992.
33. Guedez, L., Rivera, A.M., Salloum, R., Miller, M.L., Diegmueller, J.J., Bungay, P.M., and Stetler-Stevenson, W.G. Quantitative assessment of angiogenic responses by the directed *in vivo* angiogenesis assay. Am. J. Pathol. **162,** 1431, 2003.
34. Roedersheimer, M., West, J., Huffer, W., Harral, J., and Benedict, J. A bone-derived mixture of TGFbeta-superfamily members forms a more mature vascular network than bFGF or TGF-beta2 *in vivo*. Angiogenesis **8,** 327, 2005.
35. Kowalski, J., Kwan, H.H., Prionas, S.D., Allison, A.C., and Fajardo, L.F. Characterization and applications of the disc angiogenesis system. Exp. Mol. Pathol. **56,** 1, 1992.
36. Mikos, A.G., Sarakinos, G., Lyman, M.D., Ingber, D.E., Vacanti, J.P., and Langer, R. Prevascularization of porous biodegradable polymers. Biotechnol. Bioeng. **42,** 716, 1993.
37. Laschke, M.W., Harder, Y., Amon, M., Martin, I., Farhadi, J., Ring, A., Torio-Padron, N., Schramm, R., Rucker, M., Junker, D., Haufel, J.M., Carvalho, C., Heberer, M., Germann, G., Vollmar, B., and Menger, M.D. Angiogenesis in tissue engineering: breathing life into constructed tissue substitutes. Tissue Eng. **12,** 2093, 2006.
38. Komori, M., Tomizawa, Y., Takada, K., and Ozaki, M. A single local application of recombinant human basic fibroblast growth factor accelerates initial angiogenesis during wound healing in rabbit ear chamber. Anesth. Analg. **100,** 830, 2005.
39. Serbedzija, G.N., Flynn, E., and Willett, C.E. Zebrafish angiogenesis: a new model for drug screening. Angiogenesis **3,** 353, 1999.
40. Ny, A., Autiero, M., and Carmeliet, P. Zebrafish and Xenopus tadpoles: small animal models to study angiogenesis and lymphangiogenesis. Exp. Cell Res. **312,** 684, 2006.
41. Stoletov, K., Montel, V., Lester, R.D., Gonias, S.L., and Klemke, R. High-resolution imaging of the dynamic tumor cell vascular interface in transparent zebrafish. Proc. Natl. Acad. Sci. USA **104,** 17406, 2007.
42. Glowacki, J. Angiogenesis in fracture repair. Clin. Orthop. Relat. Res. **Suppl 355,** S82, 1998.
43. Kaigler, D., Wang, Z., Horger, K., Mooney, D.J., and Krebsbach, P.H. VEGF scaffolds enhance angiogenesis and bone regeneration in irradiated osseous defects. J. Bone Miner. Res. **21,** 735, 2006.
44. Lee, S.J. Cytokine delivery and tissue engineering. Yonsei Med. J. **41,** 704, 2000.
45. Santana, R.B., and Trackman, P.C. Controlled release of fibroblast growth factor 2 stimulates bone healing in an animal model of diabetes mellitus. Int. J. Oral Maxillofac. Implants **21,** 711, 2006.
46. Toyota, E., Fujimoto, K., Ogasawara, Y., Kajita, T., Shigeto, F., Matsumoto, T., Goto, M., and Kajiya, F. Dynamic changes in three-dimensional architecture and vascular volume of transmural coronary microvasculature between diastolic- and systolic-arrested rat hearts. Circulation **105,** 621, 2002.
47. Wan, S.Y., Kiraly, A.P., Ritman, E.L., and Higgins, W.E. Extraction of the hepatic vasculature in rats using 3-D micro-CT images. IEEE Trans. Med. Imaging **19,** 964, 2000.
48. Ortiz, M.C., Garcia-Sanz, A., Bentley, M.D., Fortepiani, L.A., Garcia-Estan, J., Ritman, E.L., Romero, J.C., and Juncos, L.A. Microcomputed tomography of kidneys following chronic bile duct ligation. Kidney Int. **58,** 1632, 2000.
49. Garcia-Sanz, A., Rodriguez-Barbero, A., Bentley, M.D., Ritman, E.L., and Romero, J.C. Three-dimensional microcomputed tomography of renal vasculature in rats. Hypertension **31,** 440, 1998.
50. Duvall, C.L., Robert Taylor, W., Weiss, D., and Guldberg, R.E. Quantitative microcomputed tomography analysis of collateral vessel development after ischemic injury. Am. J. Physiol. Heart Circ. Physiol. **287,** H302, 2004.
51. Duvall, C.L., Weiss, D., Robinson, S.T., Alameddine, F.M., Guldberg, R.E., and Taylor, W.R. The role of osteopontin in recovery from hind limb ischemia. Arterioscler. Thromb. Vasc. Biol. **28,** 290, 2007.
52. Hedberg, E.L., Kroese-Deutman, H.C., Shih, C.K., Lemoine, J.J., Liebschner, M.A., Miller, M.J., Yasko, A.W., Crowther, R.S., Carney, D.H., Mikos, A.G., and Jansen, J.A. Methods: a comparative analysis of radiography, microcomputed tomography, and histology for bone tissue engineering. Tissue Eng. **11,** 1356, 2005.
53. Cowan, C.M., Aghaloo, T., Chou, Y.F., Walder, B., Zhang, X., Soo, C., Ting, K., and Wu, B. MicroCT evaluation of three-dimensional mineralization in response to BMP-2 doses *in vitro* and in critical sized rat calvarial defects. Tissue Eng. **13,** 501, 2007.
54. Hokugo, A., Sawada, Y., Hokugo, R., Iwamura, H., Kobuchi, M., Kambara, T., Morita, S., and Tabata, Y. Controlled release of platelet growth factors enhances bone regeneration at rabbit calvaria. Oral Surg. Oral Med. Oral Pathol. Oral Radiol. Endod. **104,** 44, 2007.
55. Patel, Z.S., Young, S., Tabata, Y., Jansen, J.A., Wong, M., and Mikos, A.G. Dual delivery of an angiogenic and an osteogenic growth factor for bone regeneration in a critical size defect model. Bone 2008, in press.
56. Rai, B., Oest, M.E., Dupont, K.M., Ho, K.H., Teoh, S.H., and Guldberg, R.E. Combination of platelet-rich plasma with polycaprolactone-tricalcium phosphate scaffolds for segmental bone defect repair. J. Biomed. Mater. Res. A **81,** 888, 2007.
57. Bentley, M.D., Ortiz, M.C., Ritman, E.L., and Romero, J.C. The use of microcomputed tomography to study microvasculature in small rodents. Am. J. Physiol. Regul. Integr. Comp. Physiol. **282,** R1267, 2002.
58. Hedberg, E.L., Kroese-Deutman, H.C., Shih, C.K., Crowther, R.S., Carney, D.H., Mikos, A.G., and Jansen, J.A. *In vivo* degradation of porous poly(propylene fumarate)/poly(DL-lactic-co-glycolic acid) composite scaffolds. Biomaterials **26,** 4616, 2005.
59. Hedberg, E.L., Kroese-Deutman, H.C., Shih, C.K., Crowther, R.S., Carney, D.H., Mikos, A.G., and Jansen, J.A. Effect of varied release kinetics of the osteogenic thrombin peptide TP508 from biodegradable, polymeric scaffolds on bone formation *in vivo*. J. Biomed. Mater. Res. A **72,** 343, 2005.
60. Blum, J.S., Barry, M.A., Mikos, A.G., and Jansen, J.A. *In vivo* evaluation of gene therapy vectors in *ex vivo*-derived marrow stromal cells for bone regeneration in a rat critical-size calvarial defect model. Hum. Gene. Ther. **14,** 1689, 2003.

61. Dean, D., Wolfe, M.S., Ahmad, Y., Totonchi, A., Chen, J.E., Fisher, J.P., Cooke, M.N., Rimnac, C.M., Lennon, D.P., Caplan, A.I., Topham, N.S., and Mikos, A.G. Effect of transforming growth factor beta2 on marrow-infused foam poly(propylene fumarate) tissue-engineered constructs for the repair of critical-size cranial defects in rabbits. Tissue Eng. **11,** 923, 2005.
62. Jansen, J.A., Vehof, J.W., Ruhe, P.Q., Kroeze-Deutman, H., Kuboki, Y., Takita, H., Hedberg, E.L., and Mikos, A.G. Growth factor-loaded scaffolds for bone engineering. J. Control. Release **101,** 127, 2005.
63. Ruhe, P.Q., Hedberg, E.L., Padron, N.T., Spauwen, P.H., Jansen, J.A., and Mikos, A.G. Biocompatibility and degradation of poly(DL-lactic-co-glycolic acid)/calcium phosphate cement composites. J. Biomed. Mater. Res. A **74,** 533, 2005.
64. Young, S., Bashoura, A.G., Borden, T., Baggett, L.S., Jansen, J.A., Wong, M., and Mikos, A.G. Development and characterization of a rabbit alveolar bone nonhealing defect model. J. Biomed. Mater. Res. A **86,** 182, 2008.
65. Niimi, H. Cerebral angiogenesis induced by growth factors: intravital microscopic studies using models. Clin. Hemorheol. Microcirc. **29,** 149, 2003.
66. Druecke, D., Langer, S., Lamme, E., Pieper, J., Ugarkovic, M., Steinau, H.U., and Homann, H.H. Neovascularization of poly(ether ester) block-copolymer scaffolds *in vivo*: long-term investigations using intravital fluorescent microscopy. J. Biomed. Mater. Res. A **68,** 10, 2004.
67. Prokop, M., Shin, H.O., Schanz, A., and Schaefer-Prokop, C.M. Use of maximum intensity projections in CT angiography: a basic review. Radiographics **17,** 433, 1997.
68. Norrby, K. *In vivo* models of angiogenesis. J.Cell. Mol. Med. **10,** 588, 2006.
69. Grabherr, S., Djonov, V., Yen, K., Thali, M.J., and Dirnhofer, R. Postmortem angiography: review of former and current methods. Am. J. Roentgenol. **188,** 832, 2007.
70. Seo, Y., Hashimoto, T., Nuki, Y., and Hasegawa, B.H. *In vivo* microCT imaging of rodent cerebral vasculature. Phys. Med. Biol. **53,** N99, 2008.
71. Badea, C.T., Fubara, B., Hedlund, L.W., and Johnson, G.A. 4-D micro-CT of the mouse heart. Mol. Imaging **4,** 110, 2005.

Address reprint requests to:
Antonios G. Mikos, Ph.D.
Department of Bioengineering
Rice University
P.O. Box 1892, MS 142
Houston, TX 77251

E-mail: mikos@rice.edu

Received: March 10, 2008
Accepted: May 9, 2008